

# Raman scattering by surface polaritons in a GaP crystal: dispersion, intensity, and polarization properties

V. N. Denisov, B. N. Mavrin, and V. B. Podobedov

*Institute of Spectroscopy, Academy of Sciences of the USSR, Moscow*

(Submitted 10 November 1986)

Zh. Eksp. Teor. Fiz. **92**, 1855–1867 (May 1987)

A description is given of the method for the excitation and recording of the spectra of the Raman scattering by surface polaritons, which is based on the use of a pulsed laser with a high repetition frequency, a triple polychromator, and a multichannel recording system. The spectra of the Raman scattering by surface polaritons were obtained throughout the full region of the polariton dispersion of GaP. It was found that the Raman scattering intensity decreased more than tenfold as a result of the polariton shift toward the transverse phonon frequency. An analysis was made of the polarization properties of the spectra of the Raman scattering by surface polaritons, and by *TO* and *LO* phonons at low scattering angles. It was found that for certain scattering geometries when the polarizations of the exciting and scattered light were mutually perpendicular, it was possible to improve greatly the contrast in the observation of surface polaritons in Raman spectra.

## 1. INTRODUCTION

One of the most active fields in modern physics is the study of the properties of surfaces of solids because the physical properties of surfaces determine the successful use of materials in various branches of the modern technology. An important place in the studies of the surfaces and surface layers is occupied by surface optical phonons and the associated surface polaritons.

Surface phonon polaritons or briefly surface polaritons appear at an interface between two media and represent mixed excitations formed by an electromagnetic field and mechanical vibrations of a surface phonon.<sup>1,2</sup> The amplitudes of their fields decrease exponentially away from the boundary. Therefore, the propagation of surface polaritons is possible only along a boundary (and the wave vector of a surface polariton is parallel to the boundary); moreover, the maximum of the intensity of the electric field is located on the surface. Consequently, surface polaritons are sensitive to the state of a surface.

The majority of the investigations of surface polaritons have been carried out by optical methods among which an important place is occupied by a modified method of frustrated total internal reflection (FTIR) in the infrared range. The FTIR method can be used to excite surface polaritons which are, generally speaking, nonradiative oscillations and, consequently, this method can be used to determine the infrared absorption spectra of surface polaritons. However, interpretation of the FTIR data is complicated by this distorting influence of an FTIR prism on surface excitations. This shortcoming can be avoided by investigating infrared reflection spectra of surfaces on which gratings are deposited, but in this case the investigated surface is disturbed to some extent. A direct study of surface polaritons on unperturbed surfaces is possible by the Raman scattering method.

In contrast to the FTIR method, in which the wave vector of surface polaritons that can be studied has an upper limit (Chap. I in Ref. 2), the Raman scattering method does not impose such restrictions. However, the intensity of the Raman scattering by surface polaritons is very weak. Therefore, the Raman spectra of surface polaritons have been re-

corded only for a few samples [film of GaAs on Al<sub>2</sub>O<sub>3</sub> (Ref. 3), GaP (Ref. 4), NaClO<sub>2</sub> (Ref. 5), and ZnTe (Ref. 6)] in a narrow dispersion range and practically in all cases the signal/noise ratio was small. A theoretical analysis of the characteristics of Raman scattering by surface polaritons were published well before the experimental capabilities demonstrated in Refs. 3–6. Agranovich predicted a number of interesting effects<sup>1</sup> but their detection and study would require considerable improvements in the experimental technique.

Our task was to develop a method for recording the Raman spectra of surface polaritons with a good signal/noise ratio (Sec. 2) and to apply this method to study surface polaritons practically throughout the polariton dispersion region (Sec. 3.1) and the frequency dependence of the intensity of the Raman scattering by surface polaritons (Sec. 3.2), and also to carry out polarization measurements on the Raman spectra of surface polaritons with given and arbitrary directions of the surface polariton wave vector (Sec. 3.3) in a free crystalline film of GaP.

## 2. EXPERIMENTAL METHOD

The recent progress in the techniques used to record the spontaneous Raman scattering spectra, particularly those of low intensity, has depended largely on the use of multichannel recording systems. However, their advantages in the low-frequency part of the spectrum, where surface polaritons have to be studied, can be realized only if the spectroscopic instruments have sufficiently high characteristics, the principal ones being the level of stray scattered light, spectral resolution, transmission, etc. In the case of one-channel Raman spectrometers these characteristics are ensured by double or triple monochromators which, because of a number of specific properties, cannot be utilized effectively in multichannel recording systems.

We shall report the use of a "home-made" polychromator consisting of a premonochromator with dispersion subtraction and a spectrograph. The optical system of the premonochromator included two Czerny-Turner mono-

chromators and was arranged in such a way that both diffraction gratings (600 lines/mm) were on a common rotation axis and the necessary optical geometry was ensured by four concave spherical ( $F = 500$  mm) mirrors and four rotatable mirrors. All the mirrors had dielectric coatings with a high reflection coefficient in the range 400–750 nm. An intermediate slit of the premonochromator selected the working part of the spectrum within 25 nm. The premonochromator could be used in conjunction with spectrographs in which the entry slit was located horizontally or vertically. The spectrograph used in this polychromator contained only one concave holographic grating (Jobin-Yvon, type IV, 2000 lines/mm) and one rotatable mirror. The spectral range could be set in this spectrograph independently of the premonochromator. The transmission of the polychromator at  $\lambda = 532$  nm was 35 and 25% for two orthogonal polarizations and the level of scattered light was  $< 10^{-11}$  at  $50$   $\text{cm}^{-1}$  from the exciting line when the working part of the spectrum was  $50$   $\text{cm}^{-1}$ . The instrumental function of the spectrometer together with the recording system amounted to  $\sim 2$   $\text{cm}^{-1}$ .

According to Ref. 2 (Chap. 12) the expected intensity of the Raman scattering by surface polaritons does not exceed  $\sim 1$ – $10$  photoelectrons/sec. Such intensities can readily be recorded by a multichannel system used by us earlier in an experimental study of the hyper-Raman scattering of light.<sup>7</sup> Bearing in mind the specific geometry for the observation of Raman scattering by surface polaritons, particularly the small dimensions of the illuminated part of a sample, we reduced the height of photometric analysis of spectral lines to  $\sim 0.5$  mm, so as to improve the signal/noise ratio. An analysis of the spectral information and the necessary (model) calculations were carried out on an Iskra-226 computer which was linked to an F36 measuring-computing system via a functional interface controlled by an external synchronization signal from F36. The accumulation of weak optical spectra and their primary analysis was carried out in F36 and then the Raman spectra as well as the reference frequencies were stored in the memory of the Iskra-226 computer.

Surface polaritons were observed in GaP in the "forward" scattering scheme using ring diaphragms.<sup>7</sup> Diaphragms with a ring gap width  $\sim 0.5$  mm, ensuring an angular resolution  $\Delta\theta \approx 0.1^\circ$ , were located at a distance 249 mm from the sample on the axis of laser radiation transmitted at right-angles to the film surface. A set of diaphragms with different diameters of the ring gap covered the required range of angles  $\theta$  ( $1$ – $3^\circ$  outside the crystal). The Raman spectra of surface polaritons were excited by the second harmonic of a pulsed  $\text{Nd}^{3+}$  laser ( $\tau_p \approx 70$  nsec,  $F_{\text{rep}} \approx 5$  kHz). The average laser radiation power was  $\sim 1$  W, but to prevent surface damage of a sample only 100–150 mW of this power was used. The energy of the exciting ( $2.33$  eV) and scattered ( $\sim 2.28$  eV) photons was less than the indirect gap of GaP ( $2.34$  eV).

Samples of crystalline GaP films were prepared from an oriented single crystal by optical-grade grinding. The final polishing of the surface was carried out using a diamond micropowder (ASM 05/0) with a grain diameter  $\leq 0.5$   $\mu$ . Our samples were  $11 \pm 2$   $\mu$  thick and the surface was located in a (111) plane. X-ray investigations were used to find the directions  $[\bar{1}\bar{1}0]$  and  $[\bar{1}\bar{1}2]$  on the film surface. Three mutually perpendicular directions ( $x = [\bar{1}\bar{1}0]$ ,  $y = [\bar{1}\bar{1}2]$ , and

$z = [111]$ ) were selected as the Cartesian coordinate system.

Gallium phosphide is a semiconductor of the cubic symmetry  $T_d^2$ , which has the zincblende structure. Its optical vibration spectrum consists of one dipole vibration  $F_2$  which appears in the Raman spectra as a  $TO$ - $LO$  doublet characterized by a splitting of about  $36$   $\text{cm}^{-1}$  (Ref. 8). It is known<sup>1,2</sup> that the frequencies of surface polariton bands lie between the transverse ( $TO$ ) and longitudinal ( $LO$ ) phonons. We therefore investigated the Raman spectra solely in the range  $350$ – $450$   $\text{cm}^{-1}$ , where the  $TO$ - $LO$  doublet of a GaP crystal was located.

### 3. EXPERIMENTAL RESULTS AND DISCUSSION

#### 3.1. Raman spectra and dispersion of surface polaritons in a GaP crystal

Since the spectra of the Raman scattering by surface polaritons had been investigated earlier<sup>4</sup> only at larger scattering angles  $\theta$ , we concentrated our attention on the discovery of surface polaritons in the range  $\theta \leq 2^\circ$  ( $\theta$  is the scattering angle outside the crystal). The spectra of the Raman scattering by surface polaritons in a GaP film obtained for different angles are given in Figs. 1b–1j. For comparison, we included also the Raman spectrum of the same film obtained in the reflection geometry ( $\theta = 135^\circ$ , Fig. 1a). In this geom-

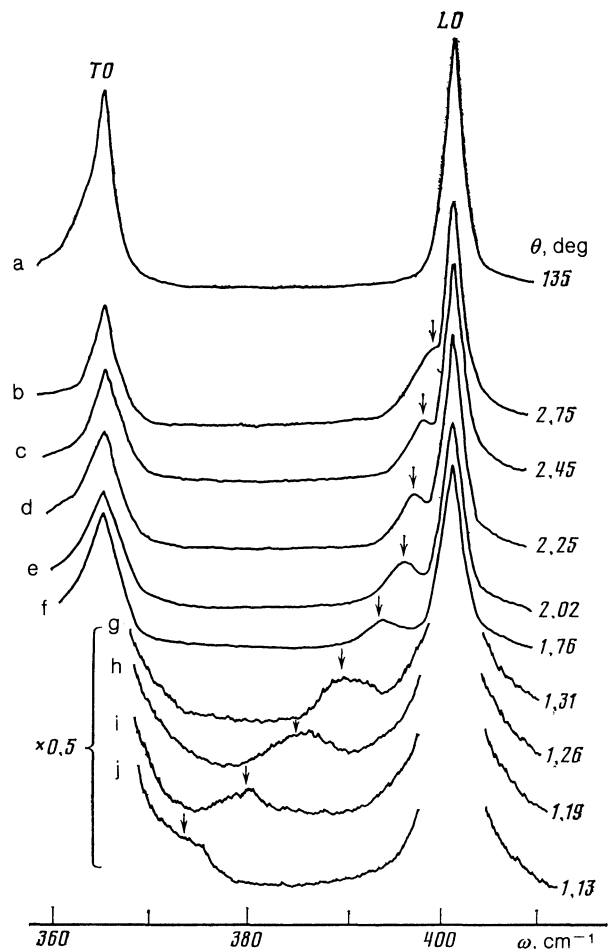


FIG. 1. Raman scattering spectra of a GaP crystal obtained for different scattering angles  $\theta$ . The arrows identify the positions of the surface polariton maxima.

etry the intensity of the Raman scattering by surface excitations was extremely low<sup>2</sup> and the spectrum consisted of just two bands which were attributed to *TO* and *LO* phonons, respectively.

At low angles  $\theta$  a maximum appeared (Fig. 1b) in the low-frequency wing of the *LO* band and its frequency decreased on reduction of  $\theta$  from 398 cm<sup>-1</sup> for  $\theta = 2.75^\circ$  to 373 cm<sup>-1</sup> for  $\theta = 1.13^\circ$ . The appearance of this maximum at low angles  $\theta$  in the region between  $\omega_{TO}$  and  $\omega_{LO}$ , and the dependence of its position on  $\theta$  were clear indication that it was due to surface polaritons. In the range  $\theta < 2^\circ$  the surface polariton line broadened considerably on reduction in  $\theta$ . In the range  $\theta < 1.13^\circ$  there was no scattering by surface polaritons. The frequency dependence of the position of the surface polariton on  $\theta$  is shown in Fig. 2. This figure includes also the results of previous investigations<sup>4</sup> of a GaP film subjected to the same surface treatment as in the present study. Therefore, whereas in Ref. 4 a change in the frequency of surface polaritons was observed only in an interval  $\sim 6$  cm<sup>-1</sup> (392–398 cm<sup>-1</sup>), in the present study this interval was broadened to 373–398 cm<sup>-1</sup> and, in fact, covered the whole dispersion range of surface polaritons.

An increase in the scattering angle  $\theta$  caused the surface polariton frequency to approach a certain limit (Fig. 2), which was close to the frequency  $\omega_s$  of a surface phonon in GaP given for the crystal-vacuum interface by the relationship<sup>1,2</sup>

$$\omega_s^2 = \omega_{TO}^2 \frac{1 + \epsilon_0}{1 + \epsilon_\infty} \quad (1)$$

( $\epsilon_0$  and  $\epsilon_\infty$  are the values of the permittivity in the limits of zero and infinite frequencies). Since the depth of penetration of the exciting radiation ( $\sim 100 \mu$ ) was greater than the film thickness, the Raman spectrum should include contributions from both boundaries of the film. When the surface waves from both boundaries interacted, the polariton spectrum should exhibit two branches and the surface polariton dispersion should differ from that for a crystal with one boundary. In the case of one boundary (crystal-vacuum) the dispersion of surface polaritons  $\omega(k_{\parallel})$  satisfies the equation<sup>1,2</sup>

$$k_{\parallel}^2 = 4\pi^2 \omega^2 \epsilon / (1 + \epsilon), \quad (2)$$

where  $k_{\parallel}$  is the wave vector of surface polaritons directed parallel to the surface ( $k_{\parallel} = k_s \sin \theta$ ,  $k_s$  is the wave vector of the scattered radiation),  $\omega$  is the surface polariton frequency (cm<sup>-1</sup>), and  $\epsilon$  is the permittivity of the crystal. The position of the polariton band in the Raman spectra was determined from the value of  $\epsilon(\omega)$  without allowance for damping.<sup>9</sup> Assuming that in the case of GaP

$$\epsilon = \epsilon_\infty + S \omega_{TO}^2 / (\omega_{TO}^2 - \omega^2), \quad (3)$$

where  $\epsilon_\infty = 0.091$ ,  $S = 1.93$ , and  $\omega_{TO} = 365.5$  cm<sup>-1</sup>, we could calculate the dispersion  $\omega(k_{\parallel})$  (continuous curve in Fig. 2). It can be seen from Fig. 2 that the experimental points lie close to the calculated curve, indicating the absence of a significant interaction of the surface waves from the two boundaries of the film. This was not surprising because in contrast to the exciting radiation the depth of penetration of surface polaritons was<sup>1,2</sup>

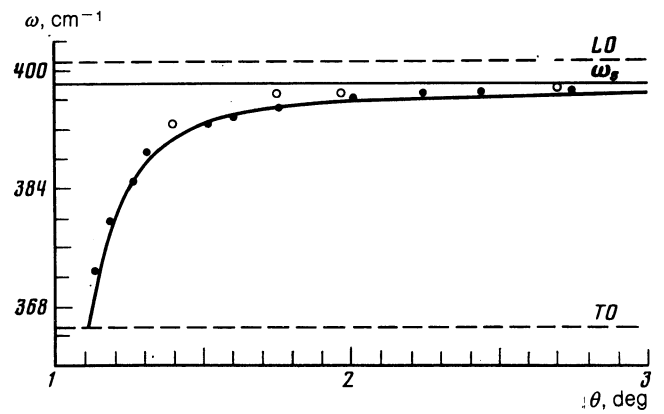


FIG. 2. Dispersion of surface polaritons in a GaP crystal: ●) our data; ○) data from Ref. 4; the continuous curve is the theoretical dispersion of Eq. (2).

$$d \approx \alpha^{-1} = (k_{\parallel}^2 - 4\pi^2 \epsilon \omega^2)^{-1/2}, \quad (4)$$

which did not exceed  $2 \mu$  for GaP (Fig. 3) and was five times less than the thickness of the film. Clearly, in this case one should regard the process of the Raman scattering by the two boundaries separately and the Raman spectra should manifest the total intensity of the Raman scattering by the two boundaries.

A calculation of the dispersion of  $\omega(k_{\parallel})$  indicated (Fig. 2) that the surface polariton branch terminating at the frequency  $\omega_{TO}$  reached this frequency at  $\theta = 1.1^\circ$ . This accounted for the absence of the Raman scattering by surface polaritons in the range  $\theta < 1.13^\circ$  in the case of GaP. In connection with investigations of the influence of a rough surface on the dispersion of surface polaritons<sup>4</sup> one should mention that we did not observe such a discrepancy between the calculated  $\omega(k_{\parallel})$  curve and the experimental results which was reported in Ref. 4.

### 3.2. Intensity of the Raman scattering by surface polaritons in a GaP crystal

Observation of the surface polariton spectra in a wide dispersion region allowed us to study for the first time the behavior of the intensity of the Raman scattering by surface polaritons when the polariton frequency was varied. It is clear from Fig. 1 that the scattering intensity fell on reduction in the angle  $\theta$ . Clearly, this was the reason why only a small shift of the surface polariton frequency ( $\sim 6$  cm<sup>-1</sup>) was observed in the case of GaP. Measurements of the polar-

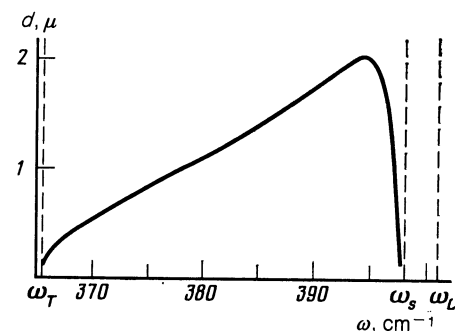


FIG. 3. Frequency dependence of the depth of penetration of surface polaritons in a GaP crystal.

iton scattering intensity were difficult to carry out because of the need to consider the angular instrumental function  $\varphi(\omega)$  for polaritons, so that the observed polariton profile  $J(\omega)$  was a convolution of three functions:

$$J(\omega) = J_0(\omega) \otimes A(\omega) \otimes \varphi(\omega), \quad (5)$$

where  $J_0(\omega)$  is the true profile and  $A(\omega)$  is the instrumental function of the spectrometer.<sup>10</sup> However, in the present study the task of determining the true intensities of surface polaritons was made easier by the fact that sufficiently accurate data were available on the functions  $A(\omega)$  and  $\varphi(\omega)$  and there was also some information on  $J_0(\omega)$ .

The  $A(\omega)$  contour could be determined experimentally and the width of  $\varphi(\omega)$ , governed by the angle of collection  $\Delta\theta$  and the nature of the dispersion of  $\omega(k_{\parallel})$ , could be calculated from the experimental dependence  $\omega(\theta)$ . Assuming that within the small limits of the angle  $\Delta\theta$  ( $\Delta\theta \approx 0.1^\circ$ ) the intensity of the Raman scattering by surface polaritons was constant, we represented the contour  $\varphi(\omega)$  by a rectangle of width equal to the frequency interval  $\Delta\omega$ , corresponding to the angle  $\Delta\theta$  of the dispersion curve  $\omega(\theta)$  near the frequency  $\omega$ , i.e.,  $\Delta\omega = \omega(\theta + \Delta\theta/2) - \omega(\theta - \Delta\theta/2)$  for each angle  $\theta$ .

The  $J_0(\omega)$  profile should be Lorentzian<sup>1,2</sup> and its width in the case of the crystal-vacuum boundary was determined as follows:

$$\Gamma(\omega) = \frac{S\omega_{TO}^2\omega^2\Gamma_{TO}(\omega)}{\epsilon_\infty(1+\epsilon_\infty)(\omega_s^2-\omega^2)^2+S\omega_{TO}^2\omega_s^2}, \quad (6)$$

where  $\Gamma_{TO}(\omega)$  is the transverse phonon damping. Since the function  $\Gamma_{TO}(\omega)$  of GaP had been investigated earlier,<sup>11</sup> it could be found in the range of frequencies of interest to us employing a many-oscillator model proposed in Ref. 11 for the optimal description of the damping  $\Gamma_{TO}(\omega)$  (Fig. 4, dashed curve). We then calculated the damping  $\Gamma(\omega)$  of a surface polariton (continuous curve in Fig. 4). In general, the damping  $\Gamma(\omega)$  decreased strongly in the limit  $\omega \rightarrow \omega_{TO}$  (Refs. 1 and 2). However, in the case of GaP an increase in  $\Gamma_{TO}(\omega)$  in the limit  $\omega \rightarrow \omega_{TO}$  (Fig. 4) had the effect that  $\Gamma(\omega)$  varied little throughout the polariton dispersion region. Therefore, had the integrated intensity of the Raman scattering by surface polaritons been constant throughout the dispersion region, the peak intensity would have increased only slightly as a result of the shift of the polariton from  $\omega_s$  to  $\omega = 373 \text{ cm}^{-1}$  because of a small reduction in  $\Gamma(\omega)$  in this region (Fig. 5a).

Next, allowing for the real functions  $A(\omega)$  and  $\varphi(\omega)$ , we would expect the surface polariton profiles [convolution of Eq. (5)] obtained for different values of  $\omega$  to have the

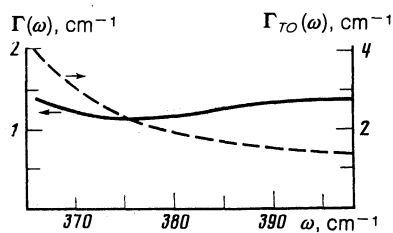


FIG. 4. Frequency dependence of the damping of a transverse phonon (dashed curve) and of a surface polariton (continuous curve) in a GaP crystal.

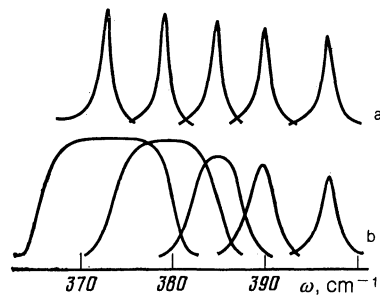


FIG. 5. Profiles calculated for surface polaritons in a GaP crystal at different frequencies: a) actual  $J_0(\omega)$  profile; b) convolutions of  $J(\omega)$ .

form shown in Fig. 5b. It is worth noting the proposed behavior of the peak intensities of the contours  $J(\omega)$  calculated on the assumption of a constant Raman scattering cross section of surface polaritons: these profiles increase only slightly as a result of displacement of a polariton from  $\omega_s$  to  $\omega = 373 \text{ cm}^{-1}$ . A relatively slight distortion of the peak intensities of the true profiles  $J_0(\omega)$  (Fig. 5a) by the instrumental functions  $A(\omega)$  and  $\varphi(\omega)$  was due to the fact that the widths of the surface polariton profiles [ $\Gamma(\omega)$ ] were less than the widths of the instrumental functions and, moreover, they varied little with frequency.

The results of these calculations (Fig. 5), based on the actual dependences  $A(\omega)$ ,  $\varphi(\omega)$ , and  $\Gamma(\omega)$ , were used to find the cross section of the Raman scattering by surface polaritons using the peak intensities  $I_p(\omega)$  of the observed surface polariton bands (Fig. 1). The values of  $I_p(\omega)$  were deduced from the absolute measurements because the intensities of the *TO* and *LO* phonons could not always be used as the internal standard of the intensity in thin films. We estimated the error of measurements carried out in this way to be  $\sim 20\%$  in the range 393–397  $\text{cm}^{-1}$ . A reduction in the frequency resulted in an increase in this error, which reached  $\sim 50\%$  at 373  $\text{cm}^{-1}$ . In the determination of the cross section for the Raman scattering at different angles  $\theta$  from the measured values of  $I_p(\omega)$  we should include a small correction the  $I_p(\omega)$  data in accordance with Fig. 5b. We established that the intensity of the Raman scattering by surface polaritons in GaP had a maximum near 396.5  $\text{cm}^{-1}$  and decreased more than tenfold on reduction in the frequency to 373  $\text{cm}^{-1}$  (points in Fig. 6).

We shall now consider the theoretical frequency dependences of the cross section for the Raman scattering by surface polaritons. According to Ref. 2 (Chap. 12) this cross section of the crystal-vacuum interface is described by

$$I(\omega) \approx |\chi|^2 \Phi(\omega) = |\chi|^2 \frac{\omega_s^3 \cos^2 \theta \alpha_0 (|\alpha|^2 + k_{\parallel}^2)}{|\alpha| (|k_i^z - k_s^z|^2 + |\alpha'|^2)} \text{Im} \left( \frac{1}{\alpha + \epsilon \alpha_0} \right) \quad (7)$$

Equation (7) includes only the terms which depend on the polariton frequency  $\omega$ . Here,  $\chi$  is the effective susceptibility for the Raman scattering;  $\alpha_0 = (k_{\parallel}^2 - 4\pi^2\omega^2)^{1/2}$ ,  $\alpha = \alpha' + i\alpha''$ ;  $k_i^z$  and  $k_s^z$  are the components of the wave vectors of the incident and scattered light along the *z* axis, perpendicular to the film surface. Since we drew the attention earlier only to a strong reduction in the Raman scattering intensity by surface vibrations in the case of backscatter-

ing, compared with the forward scattering, we carried out a numerical analysis of Eq. (7) at low angles  $\theta$ . If in the first approximation we adopt  $|\chi|^2 = \text{const}$ , we find that the dependence  $I(\omega)$  is identical with the function  $\Phi(\omega)$ . Therefore, we shall first analyze  $\Phi(\omega)$ . For clarity, we shall normalize all the functions  $I(\omega)$  to the maximum of the experimental dependence (Fig. 6).

In a numerical analysis of the function  $\Phi(\omega)$  for GaP it is found that it has a maximum in the polariton dispersion region and, moreover, that  $\Phi(\omega) \rightarrow 0$  if  $\omega \rightarrow \omega_{TO}$  and also if  $\omega \rightarrow \omega_s$ . The main reason for this behavior of  $\Phi(\omega)$  is the change in the depth  $d$  of the penetration of surface polaritons [Eq. (4)] which is a function of the polariton frequency. We can see from Fig. 3 that in the case of GaP the maximum depth is  $d_{\text{max}} \approx 2 \mu$  at  $395 \text{ cm}^{-1}$  and we reach the limit  $d \rightarrow 0$  for  $\omega \rightarrow \omega_{TO}, \omega_s$ . In the limit  $\omega \rightarrow \omega_s$ , when the angle  $\theta$  rises strongly, the reduction in  $\Phi(\omega)$  is again due to an increasing contribution of the term  $|k_i^z - k_s^z|^2$  in the denominator of Eq. (7).

The nature of the function  $\Phi(\omega)$  is sensitive to the selection of the permittivity function  $\varepsilon(\omega)$ , which in this case should allow also for the damping of  $TO$  phonons. In the simplest case of one-oscillator model<sup>11</sup> for which  $\varepsilon(\omega)$  has the form of Eq. (3) allowing for the damping  $\Gamma = 1.28 \text{ cm}^{-1}$ , the maximum of  $\Phi(\omega)$  occurs at a lower frequency than the experimental maximum and the width of the contour  $\Phi(\omega)$  is twice as large as the experimental one (Fig. 6a). If we use a more rigorous description of  $\varepsilon(\omega)$  by the many-oscillator model,<sup>11</sup> we find that the function  $\Phi(\omega)$  is close to the experimental dependence in the range  $\omega > 393 \text{ cm}^{-1}$ . However, if  $\omega < 393 \text{ cm}^{-1}$ , the predicted reduction in the intensity is more rapid than that found experimentally (Fig. 6b).

A comparison of  $\Phi(\omega)$  with the experimental values of  $I(\omega)$  is not quite correct because we know that the value of  $|\chi|^2$  cannot be constant in the dispersion region of surface polaritons, but has a resonance reaching a maximum at  $\omega = \omega_{TO}$ . Since the dependence  $\chi(\omega)$  for a GaP crystal<sup>12</sup> had been established earlier and confirmed by the spectra of the Raman scattering on bulk polaritons, it would be natural to include it in discussing  $I(\omega)$ . In the frequency range  $398\text{--}373 \text{ cm}^{-1}$  the value of  $|\chi|^2$  rises more than tenfold on reduction in  $\omega$ . If we allow for the frequency dependence of  $|\chi|^2$ , we find that a one-oscillator model of  $\varepsilon(\omega)$  gives  $I(\omega)$  which differs very greatly from the experimental curve (Fig. 6c).

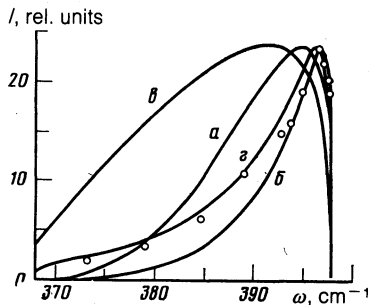


FIG. 6. Frequency dependences of the intensity of the Raman scattering by surface polaritons in GaP crystals: the points are the experimental result and the curves are theoretical; a)–d) curves calculated for  $|\chi|^2 = \text{const}$  (a, b) and  $\chi(\omega)$  in accordance with Ref. 12 (c, d); a), c) one-oscillator model of  $\varepsilon(\omega)$ ; b), d) many-oscillator model of  $\varepsilon(\omega)$ .

However, if  $\varepsilon(\omega)$  is described by a many-oscillator model the agreement between the calculated dependence  $I(\omega)$  and the experimental results is very good.

We thus found that the experimental frequency dependence of the intensity of the Raman scattering by surface polaritons in GaP is described well by the existing theoretical dependences if a consistent allowance is made for the damping  $\Gamma(\omega)$  and a rigorous description of  $\varepsilon(\omega)$  and of the nonlinearity of  $\chi(\omega)$  is used. We are of the opinion that the behavior of the intensity of the Raman scattering by surface polaritons found for a GaP crystal should be qualitatively the same for all crystals, since the main factors [resonant nature of  $\chi(\omega)$ , variation of the depth of penetration  $d$  of surface polaritons, and rise of  $|k_i^z - k_s^z|^2$  with the angle  $\theta$ ], which affect significantly the dependence  $I(\omega)$ , apply to any crystal. Deviations from such dependences can be expected only in the case of very thin films when we have to allow for the interaction of surface waves originating from the two boundaries of the film.

### 3.3. Polarization characteristics of the spectra of the Raman scattering by surface polaritons in GaP

Since a GaP film was oriented, we were able to study the state of polarization of the Raman spectra. We found it possible to improve the contrast of the surface polariton bands by polarization measurements. We first investigated (Fig. 1) depolarized spectra which demonstrated clearly that the  $LO$  phonon band increased considerably the intensity of the surface polariton bands. Therefore, it was difficult to study surface polaritons at angles  $\theta > 2^\circ$ . The ratio of the intensities of  $LO$  phonon and surface polariton bands increased even further when the polarization of the incident light ( $E_i$ ) was parallel to that of the scattered light ( $E_s$ ), as shown in Figs. 7a and 7c. However, in the ( $E_i$ ) case, the contrast of the

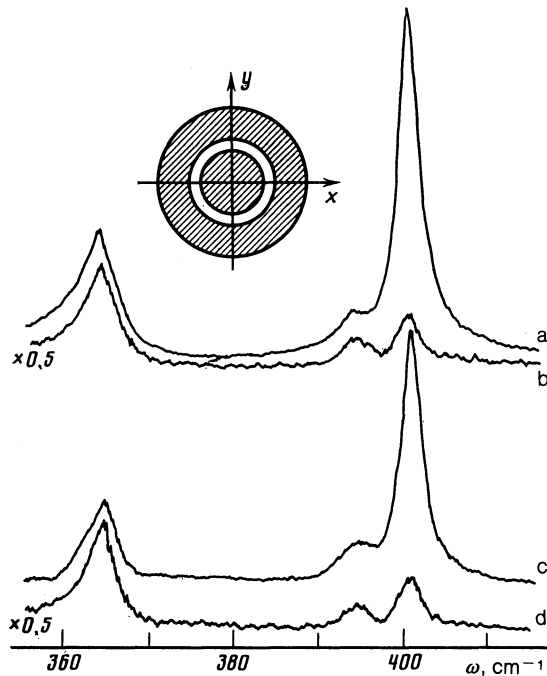


FIG. 7. Polarized Raman scattering spectra obtained for  $\theta = 1.76^\circ$  by collecting light transmitted by the whole area of the ring diaphragm (inset): a), b)  $E_i \parallel y$ ; c), d)  $E_i \parallel x$ ; a)  $z(xx)z$ ; b)  $z(xy)z$ ; c)  $z(yy)z$ ; d)  $z(yx)z$ .

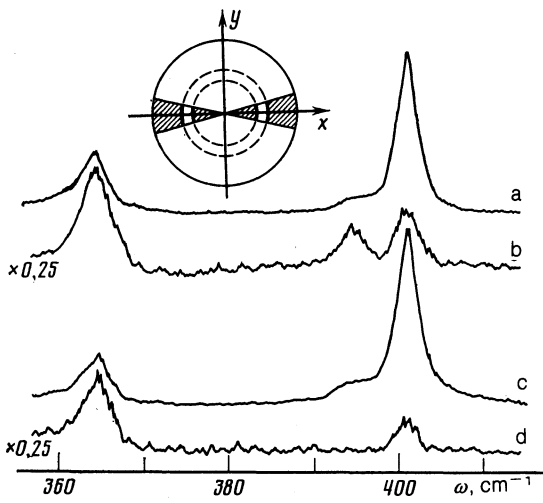


FIG. 8. Polarized Raman spectra obtained for  $\theta = 1.76^\circ$  when the scattered light was collected through a part of the ring diaphragm bounded by a sector (inset):  $\mathbf{E}_i \parallel \mathbf{x}$ ; a), b)  $\mathbf{k}_{\parallel} \parallel \mathbf{x}$ ; c), d)  $\mathbf{k}_{\parallel} \parallel \mathbf{y}$ ; a), c)  $z(xx)z$ ; b), d)  $z(xy)z$ .

surface polariton bands improved greatly and the intensities of the surface polariton and  $LO$  phonon bands became almost identical (Figs. 7b and 7d). There was also a change in the ratio of the intensities of the  $TO$  and  $LO$  phonons (Fig. 7). In the  $\mathbf{E}_i \parallel \mathbf{E}_s$  case the  $TO$  band was several times weaker than the  $LO$  band, whereas for  $\mathbf{E}_i \perp \mathbf{E}_s$  the intensity of the  $LO$  phonons fell more than tenfold. In recording these spectra (Fig. 7) we selected the directions of the polarizations  $\mathbf{E}_i$  and  $\mathbf{E}_s$ , but the orientation of the wave vectors of the scattered light and of the polariton was not determined because we were analyzing scattered light which was transmitted by the whole area of the ring diaphragm (inset in Fig. 7).

In the next experiment we limited the area of the ring diaphragm to just a sector (inset in Fig. 8). When the cut in the sector diaphragm was directed along the  $x$  axis, then a clearly the light transmitted by this diaphragm would be scattered by polaritons with the wave vector also preferentially directed along the  $x$  axis. Therefore, a sector diaphragm could be used to select any direction of the wave vectors of surface polaritons in the plane of the film ( $xy$ ). We plotted in Figs. 8 and 9 the Raman spectra for different orientations of the exciting and scattered light and for different directions of the wave vector of surface polaritons. The Raman spectra were sensitive to the selection of the scattering geometry. For example, if  $\mathbf{k}_{\parallel} \parallel \mathbf{y}$  and  $\mathbf{E}_s \perp \mathbf{E}_i$ , the intensity of the surface polariton scattering became so weak that it could not be detected experimentally, whereas for  $\mathbf{k}_{\parallel} \parallel \mathbf{x}$  and  $\mathbf{E}_i \perp \mathbf{E}_s$  the surface polariton scattering was comparable with the intensity of the  $LO$  phonon.

TABLE I. Intensities of  $TO$  and  $LO$  phonons in Raman spectra of GaP films ( $d_1 = d^2/3, d_2 = \beta^2 d_1$ ).

	$I_{xx} = I_{yy}$		$I_{xy} = I_{yx}$	
	$TO$	$LO$	$TO$	$LO$
$\mathbf{k}_{\parallel} \parallel \mathbf{x}$	$2d_1$	$d_2(1 + \cos^2 \alpha)^*$	$2d_1$	$2d_2 \sin^2 \alpha$
$\mathbf{k}_{\parallel} \parallel \mathbf{y}$	$2d_1$	$d_2(1 + \cos^2 \alpha)$	$2d_1$	0

\*Here,  $\alpha$  is the angle between the wave vectors  $\mathbf{k} = \mathbf{k}_i - \mathbf{k}_s$  and  $\mathbf{k}_i$  ( $\alpha \approx 8^\circ$  for the scattering angle  $\theta = 1.76^\circ$ ).

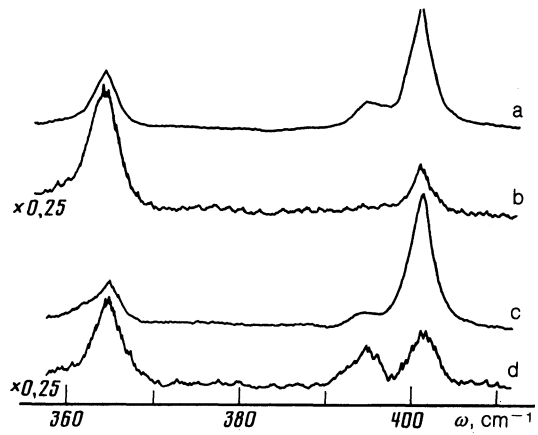


FIG. 9. Polarized Raman spectra of a GaP crystal obtained for  $\theta = 1.76^\circ$  and for light collected in the same way as in Fig. 8:  $\mathbf{E}_i \parallel \mathbf{y}$ ; a), b)  $\mathbf{k}_{\parallel} \parallel \mathbf{y}$ ; c), d)  $\mathbf{k}_{\parallel} \parallel \mathbf{x}$ ; a), c)  $z(yy)z$ ; b), d)  $z(yx)z$ .

The reasons for the observed changes in the spectra (Figs. 7–9) can be understood if we consider the selection rules for the dipole triply degenerate vibration  $F_2(x, y, z)$  of the  $T_d$  group in the Raman spectra of a film of GaP with the selected orientation. The Raman scattering tensors were obtained earlier<sup>13</sup> for this orientation, but different directions of the axes were selected in Ref. 13 and, moreover, an error was made in the calculations. Therefore, we shall give the Raman scattering tensors for the  $F_2(x, y, z)$  vibration in the coordinate system selected by us ( $x = [\bar{1}\bar{1}2]$ ,  $y = [1\bar{1}0]$ , and  $z = [111]$ ):

$$R(x) = \frac{d}{\sqrt{3}} \begin{pmatrix} 0 & -\sqrt{2} & -1 \\ -\sqrt{2} & 0 & 0 \\ -1 & 0 & 0 \end{pmatrix},$$

$$R(y) = \frac{d}{\sqrt{3}} \begin{pmatrix} -\sqrt{2} & 0 & 0 \\ 0 & \sqrt{2} & -1 \\ 0 & -1 & 0 \end{pmatrix}, \quad (8)$$

$$R(z) = \frac{d}{\sqrt{3}} \begin{pmatrix} -1 & 0 & 0 \\ 0 & -1 & 0 \\ 0 & 0 & 2 \end{pmatrix},$$

where  $d$  is the nonzero component of the Raman scattering tensor in terms of the initial axes ( $x' = [100]$ ,  $y' = [010]$ , and  $z' = [001]$ ). In the analysis of the intensities in the spectra (Figs. 7–9) it will be necessary to consider the tensors of the intensities of the  $TO$  and  $LO$  bands and of surface polariton bands.

TABLE II. Intensities of surface polaritons in Raman scattering spectra of GaP films ( $\beta' = -\alpha/k_{\parallel}$ )\*.

	$E_i \parallel x$		$E_i \parallel y$	
	$I_{xx}$	$I_{xy}$	$I_{yy}$	$I_{yx}$
$k_{\parallel} \parallel x$	$d_1$	$2d_1(\beta')^2$	$d_1$	$2d_1(\beta')^2$
$k_{\parallel} \parallel y$	$d_1(\sqrt{2}\beta' + 1)^2$	0	$d_1(\sqrt{2}\beta' - 1)^2$	0

\*Here,  $\beta'$  depends on the angle  $\theta$  and  $\beta'$  is  $-1.4$  for  $\theta = 1.76^\circ$ .

In the case of cubic crystals the intensity of the Raman scattering by dipole vibrations can be represented by<sup>14</sup>

$$I_{mn} = A \left[ \sum_{\tau} e_m^i R_{mn}(\tau) e(\tau) e_n^s \right]^2, \quad (9)$$

where  $e_m^i$  and  $e_n^s$  are the components of the unit vectors of the electric fields  $E_i$  and  $E_s$  along the directions of  $m$  and  $n$ ;  $R_{mn}(\tau)$  are the components of the Raman scattering of Eq. (8) for the phonon polarization along  $\tau$  ( $\tau = x, y, z$ );  $e(\tau)$  is a unit vector of the electromagnetic oscillation field;  $e(\tau) = e_{\parallel}(\tau)$  if the wave vector of the oscillations is parallel to  $\tau$ , and  $e(\tau) = e_{\perp}(\tau)$  if the wave vector of the oscillations is perpendicular to  $\tau$ . If the wave vector  $k$  makes an angle  $\alpha$  with the direction of  $\tau$ , then  $e(\tau) = e_{\parallel}(\tau) \cos \alpha$  and  $e(\tau) = e_{\perp}(\tau) \sin \alpha$ , respectively describe the components parallel and perpendicular to  $\tau$ .

It is known that in the case of phonons in cubic crystals we have  $e_{\parallel}(\tau) = \beta e_{\perp}(\tau)$  (for example,  $\beta = 1.4$  for GaP).<sup>15</sup> Moreover,  $e_{\parallel}(\tau)$  is responsible for the excitation of the *LO* phonons, whereas  $e_{\perp}(\tau)$  is responsible for the *TO* phonons. Using Eq. (9) we can readily analyze the intensities of the *TO* and *LO* phonons in the experimental situations discussed above (Table I). In the determination of the components  $I_{mn}$  in Table I we allowed for the fact that in the case of the forward scattering the appearance of the *TO* phonon in the Raman spectra is possible only as a result of reflection from the rear boundary of the film, because at low angles  $\theta$  instead of the *TO* phonon we should observe waveguide modes.<sup>16</sup> The intensity of the *LO* phonon is governed by two contributions: reflection from the rear surface and the forward scattering. It is clear from Table I that the *TO* phonon intensity is independent of the experimental geometry, whereas the *LO* phonon intensity for the  $E_i \parallel E_s$  polarization is considerably greater than for  $E_i \perp E_s$ . It is these features of the *TO* and *LO* bands that appear in the spectra (Figs. 7–9). In view of the finite angle of collection of the scattered light the intensity  $I_{xy}$  for the *LO* phonon for  $k_{\parallel} \parallel y$  does not vanish in the Raman spectra, although it is very small.

In an analysis of the intensity of the surface polariton band we have to allow for two factors. Firstly, the polarization of surface polaritons is elliptic and unit vectors of the axes of the ellipse  $e_{\parallel}$  and  $e_{\perp}$  (parallel and perpendicular to the film surface) lie in the sagittal plane, i.e.,  $e_{\perp} \parallel z$  and  $e_{\parallel} \parallel k_{\parallel}$  (Refs. 1 and 2). Secondly, in the case of an isotropic medium the relationship between  $e_{\parallel}$  and  $e_{\perp}$  for a surface wave is<sup>1,2</sup>

$$e_{\parallel} = -e_{\perp} \alpha / k_{\parallel} = e_{\perp} \beta'. \quad (10)$$

The intensities of the surface polariton bands in the Raman

spectra obtained for different scattering geometries had been analyzed earlier.<sup>13</sup> However, because of the inaccuracies, the results of the analysis of Ref. 13 do not correspond to the observed intensities of the surface polariton bands in the Raman spectra (Figs. 8 and 9). In particular, the analysis given in Ref. 13 predicts that if  $k_{\parallel} \parallel y$ , then the intensities  $I_{xx}$  and  $I_{yy}$  are always equal. However, this does not agree with the experimental results (Figs. 8c and 9a). Using Eqs. (9) and (10), we can find the expected intensities of the surface polariton bands for different scattering geometries (Table II). It is clear from Table II that  $I_{xx} = I_{yy}$  and  $I_{xy} = I_{yx}$  for  $k_{\parallel} \parallel x$  and also  $I_{xy} = I_{yx} = 0$  if  $k_{\parallel} \parallel y$ . However,  $I_{xx} \neq I_{yy}$  is true if  $k_{\parallel} \parallel y$ . The difference between  $I_{xx}$  and  $I_{yy}$  in the case when  $k_{\parallel} \parallel y$  depends on the angle  $\theta$  and for  $\theta = 1.76^\circ$  we can expect  $I_{yy} = 9I_{xx}$ . The theoretical characteristics of the intensities of the surface polariton bands (Table II) are in agreement with the observations (Figs. 8 and 9). It should be pointed out that such large differences between the intensities  $I_{xx}$  and  $I_{yy}$  in the case when  $k_{\parallel} \parallel y$  can be used to determine the axes  $[1\bar{1}0]$  and  $[\bar{1}\bar{1}2]$  of GaP films when their surfaces are parallel to the (111) plane.

We have discussed so far the spectra of the surface polaritons for which the wave vector is directed along the  $x$  or  $y$  axes, i.e., when the angle of collection of the scattered light is limited not only by the ring diaphragm, but reduced further to a sector of this diaphragm. Although such an investigation of the surface polariton spectra is possible (Figs. 8 and 9), a considerable fraction of the signal intensity transmitted by the whole ring diaphragm is then lost. An analysis of the scattering geometry without a sector is fundamentally the same as before. However, the process is very cumbersome because it requires integration over the whole diaphragm. Nevertheless, it is found that in this case again the intensity of the *LO* phonon for  $E_i \parallel E_s$  is considerably greater than for  $E_i \perp E_s$ , and the intensity of the *TO* phonon is the same in both polarizations. This circumstance improves the contrast in the observation of surface polaritons for  $E_i \perp E_s$ , as demonstrated in Fig. 7.

#### 4. CONCLUSIONS

The method for the excitation and recording of the Raman spectra of surface polaritons developed by us made it possible to detect polaritons practically throughout the full dispersion range of a GaP crystal. The sensitivity was sufficient to study the changes in the polariton intensity for different scattering angles. We established that this intensity decreased more than tenfold when the polariton frequency shifted from  $397 \text{ cm}^{-1}$  to  $373 \text{ cm}^{-1}$  and this was mainly due to a reduction in the depth of penetration of the surface wave

into the crystal. The existing theory of the Raman scattering by surface polaritons describes fully satisfactorily both the dispersion and the intensity of the polaritons if an allowance is made for the frequency dependences of the damping of a transverse phonon, the behavior of the permittivity is described accurately, and the resonance behavior of the nonlinear susceptibility of the Raman scattering process is taken into account. An analysis was made of the polarization relationships in the case of the spectra of the Raman scattering by surface polaritons at low scattering angles. It was found that there a scattering geometry for which the contrast of the observed surface polaritons greatly improved.

The authors are grateful to Prof. V. M. Agranovich for stimulating discussions and to A. A. Balashov for his help in the development of the premonochromator.

<sup>1</sup>V. M. Agranovich, Usp. Fiz. Nauk **115**, 199 (1975) [Sov. Phys. Usp. **18**, 99 (1975)].

<sup>2</sup>V. M. Agranovich and D. L. Mills (eds.), *Surface Polaritons: Electromagnetic Waves at Surfaces and Interfaces*, North-Holland, Amsterdam (1982) [Modern Problems in Condensed Matter Sciences, Vol. 1].

<sup>3</sup>D. J. Evans, S. Ushioda, and J. D. McMullen, Phys. Rev. Lett. **31**, 369 (1973).

<sup>4</sup>S. Ushioda, A. Aziza, J. B. Valdez, and G. Mattei, Phys. Rev. B **19**, 4012 (1979).

<sup>5</sup>G. Mattei, M. Pagannone, B. Fornari, and L. Mattioli, Solid State Commun. **44**, 1495 (1982).

<sup>6</sup>J. Watanabe, T. Sekine, K. Uchinokura, and E. Matsuura, Solid State Commun. **45**, 403 (1983).

<sup>7</sup>V. N. Denisov, B. N. Mavrin, V. B. Podobedov, and Kh. E. Sterin, Zh. Eksp. Teor. Fiz. **84**, 1266 (1983) [Sov. Phys. JETP **57**, 733 (1983)].

<sup>8</sup>B. Kh. Baïramov, Yu. É. Kitaev, V. K. Negoduiko, and Z. M. Khashkhozhev, Fiz. Tverd. Tela (Leningrad) **16**, 1129 (1974) [Sov. Phys. Solid State **16**, 725 (1974)].

<sup>9</sup>V. M. Agranovich and V. L. Ginzburg, Zh. Eksp. Teor. Fiz. **61**, 1243 (1971) [Sov. Phys. JETP **34**, 662 (1972)].

<sup>10</sup>B. N. Mavrin and Kh. E. Sterin, in: Modern Problems in Raman Scattering Spectroscopy [in Russian], Nauka, Moscow (1978), p. 48.

<sup>11</sup>A. S. Barker Jr, Phys. Rev. **165**, 917 (1968).

<sup>12</sup>W. L. Faust and C. H. Henry, Phys. Rev. Lett. **17**, 1265 (1966).

<sup>13</sup>S. Ushioda, Prog. Opt. **19**, 141 (1981).

<sup>14</sup>R. Loudon, Adv. Phys. **13**, 423 (1964).

<sup>15</sup>M. Cardona and G. Güntherodt (eds.), *Light Scattering in Solids II: Basic Concepts and Instrumentation*, Springer Verlag, Berlin (1982) [Topics in Applied Physics, Vol. 50].

<sup>16</sup>J. B. Valdez, G. Mattei, and S. Ushioda, Solid State Commun. **27**, 1089 (1978).

Translated by A. Tybulewicz